

Itinerant electronic ferromagnetism in $\text{Sr}_2\text{ScO}_3\text{CoAs}$ with largely spaced CoAs conduction layers

Hiroto Ohta,^{*} Daisuke Noguchi, Koichiro Nabetani, and Hiroko Aruga Katori[†]

*Institute of Engineering, Division of Advanced Applied Physics, Tokyo University of Agriculture and Technology,
Nakacho 2-24-16, Koganei, Tokyo 184-8588, Japan*

(Received 23 January 2013; revised manuscript received 26 August 2013; published 30 September 2013)

We studied magnetism of $\text{Sr}_2\text{ScO}_3\text{CoAs}$, a member of the group of layered compound with CoAs conducting layers, by using successfully synthesized polycrystalline sample. As a result of magnetic and electric resistivity measurements, $\text{Sr}_2\text{ScO}_3\text{CoAs}$ was revealed to be an itinerant electronic ferromagnet with the Curie temperature $T_C = 48$ K. We discussed the magnetism of this compound within the spin fluctuation theory for three-dimensional itinerant electronic ferromagnets in the ordered state and also pointed out possible quasi-two-dimensional behavior observed in magnetism.

DOI: [10.1103/PhysRevB.88.094441](https://doi.org/10.1103/PhysRevB.88.094441)

PACS number(s): 75.30.Cr, 75.50.Cc, 75.60.Ej

I. INTRODUCTION

Itinerant electronic magnetism is an old but still interesting theme in strongly correlated electronic systems. Several new topics have recently sprung from this field, e.g., iron-based η -carbide-type compounds with the *stella quadrangula* network, where itinerant electronic magnetism collaborates with a geometrical frustration,^{1,2} and UCoGe in which superconductivity and itinerant electronic ferromagnetism coexist.³⁻⁵ Collaboration between low-dimensionality and itinerant electronic magnetism is also one of the interesting topics. A group of compounds with CoPn conducting layers (Pn : P and As) has recently attracted attention as a candidate for collaboration between ferromagnetism and two-dimensionality because of their layered structure.

Among the family with CoPn conducting layers, LaCoPnO , which have the same structure as iron-based superconductor $\text{LaFeAs}(\text{O},\text{F})$,⁶ have been studied by several groups.⁷⁻⁹ In spite of a relatively large interlayer distance of CoPn layers (~ 8.5 Å), those compounds show ferromagnetism below the Curie temperature $T_C \sim 50$ K. Ferromagnetic ordering at finite temperature is an evidence of existence of magnetic interactions between CoPn layers, meaning the system is not purely two-dimensional but quasi-two-dimensional. For enhancement of two-dimensionality, it seems a good way to increase the distance between CoPn layers. $\text{Sr}_2\text{ScO}_3\text{CoPn}$ (also called as $\text{Sr}_4\text{Sc}_2\text{O}_6\text{Co}_2\text{Pn}_2$ or $\text{Sr}_2\text{ScCoPnO}_3$) are suitable compounds for such a purpose: CoPn layers are separated by a perovskitelike Sr_2ScO_3 block, and the distance between CoPn layers is therefore about 16 Å, which is a value about two times larger than that of LaCoPnO (see Fig. 1). For the case of $Pn = \text{As}$, $\text{Sr}_2\text{ScO}_3\text{CoAs}$ was reported to show a ferromagneticlike behavior with T_C possibly being higher than room temperature,¹⁰ a value that is the highest among compounds with CoPn layers. This result is surprising because enhancement of two-dimensionality usually causes a lowering of magnetic transition temperature. For further understanding of itinerant ferromagnetism in two dimensions, it is important to elucidate precise magnetism of $\text{Sr}_2\text{ScO}_3\text{CoAs}$.

Spin fluctuation is one of the most important keywords for strongly correlated electronic systems. In the case of iron-based superconductors, for example, antiferromagnetic spin fluctuations are reported to play an important role for the formation of the Cooper pairs.¹¹ Usually spin fluctuations

of compounds can be observed only by NMR and neutron-diffraction experiments.¹² For weak ferromagnets, however, one can pull out the information of spin fluctuations by measuring macroscopic (static) magnetization according to Takahashi's spin-fluctuation theory.¹³ The family with CoPn layers conforms to such a situation, since they tend to become weakly itinerant electronic ferromagnets (WIFs).

In this paper, we report results of synthesis of $\text{Sr}_2\text{ScO}_3\text{CoAs}$ and electric resistivity and magnetic measurements for our sample. We also discuss magnetism of this compound based on the spin-fluctuation theory for WIFs.^{13,14}

II. EXPERIMENT

Polycrystalline samples of $\text{Sr}_2\text{ScO}_3\text{CoAs}$ were obtained by a conventional solid-state reaction method.¹⁰ A powder of CoAs was first synthesized from powders of cobalt (purity: 99.9%) and arsenic (purity: 99.9%) by heating a mixture of them at 800 °C in evacuated silica tubes. Obtained CoAs powder was then mixed with Sr (purity: 99%), SrO (purity: 99%), and Sc_2O_3 (purity: 99.9%) in an appropriate ratio. This process was performed in a glovebox filled with highly pure N_2 gas to prevent the oxidation of Sr and moisture absorption of SrO. The mixture was sealed in a silica tube and heated at 1200 °C for two days. After regrinding, the obtained sample was heated again at 1200 °C for two days. The final process was repeated twice to homogenize the sample.

The obtained sample was characterized by powder x-ray diffraction (XRD) measurements utilizing RIGAKU Smart-Lab with $\text{Cu } K_\alpha$ radiation. Crystal structure was refined by the Rietveld method using RIETAN-FP software.¹⁵ Magnetization (M) of the sample was measured using a superconducting quantum interference device magnetometer (MPMS, Quantum Design) installed in RIKEN in conditions of temperature (T) from 2 to 300 K, and magnetic field (H) up to 70 kOe. Electric resistivity (ρ) was measured by a conventional dc four-probe method in a condition of T from 10 to 280 K with the sample sintered in a shape of a rectangle about $1 \times 2 \times 0.5$ mm³ in size.

III. RESULTS AND DISCUSSION

A. Characterization

Figure 2 shows the results of powder XRD measurement and Rietveld analysis. The simulated pattern obtained by

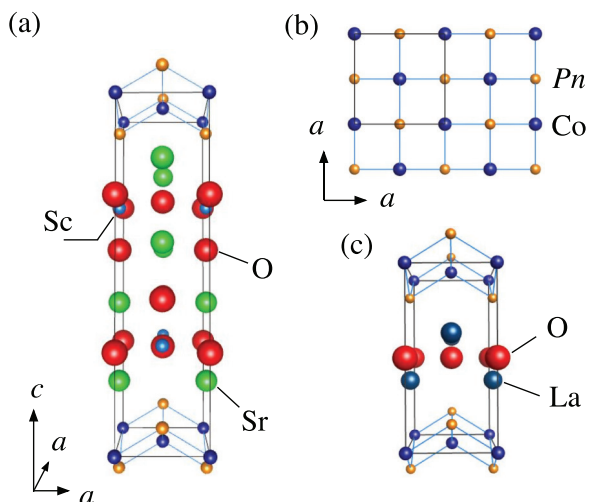


FIG. 1. (Color online) (a) Crystal structure of $\text{Sr}_2\text{ScO}_3\text{CoPn}$. (b) Projection of the CoPn conduction layers along the c axis. (c) Crystal structure of LaCoPnO shown for comparison. Two compounds belong to the tetragonal structure with space group of $P4/nmm$. Solid black lines show unit cell of each structure. Panels (a) and (c) are drawn on almost the same scale.

Rietveld analysis well explains the experimental data and no extra peak is observed, showing that the sample is in a single phase of $\text{Sr}_2\text{ScO}_3\text{CoAs}$. Lattice parameters were determined as $a = 4.0486 \text{ \AA}$ and $c = 15.557 \text{ \AA}$, which are similar to those reported by Xie *et al.*¹⁰ The result of Rietveld refinement is shown in Table I.

The value of parameter a is similar to that of LaCoAsO ($a = 4.055 \text{ \AA}$),⁹ while the value of c is about two times larger than that of LaCoAsO ($c = 8.462 \text{ \AA}$),⁹ as pointed out above. The similarity of the value of a indicates a realization of similar magnetism within the CoAs layers, since the band structures of the CoAs layer in two compounds are expected to be the same as each other. On the other hand, the difference of value of c may lead to different magnetic transition temperatures, since magnetic interaction along the c axis, which is responsible for

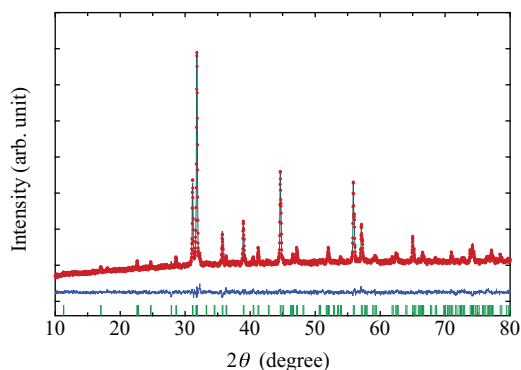


FIG. 2. (Color online) Powder XRD pattern of the sample and the result of Rietveld analysis. Upper row: Observed pattern (red dots) and simulated pattern obtained by Rietveld analysis (green line). Middle row: Difference profile between the observed and simulated patterns. Bottom row: Positions of Bragg reflections from $\text{Sr}_2\text{ScO}_3\text{CoAs}$.

TABLE I. Result of Rietveld analysis of $\text{Sr}_2\text{ScO}_3\text{CoAs}$. R_p , R_{wp} , and R_{exp} are the profile R factor, the weighted profile R factor and the expected R factor, respectively. $S = R_{wp}/R_{exp}$.

a (Å)	c (Å)	R_p (%)	R_{wp} (%)	R_{exp} (%)	S
4.0486(3)	15.557(1)	1.943	2.532	2.001	1.27
	x	y	z	occupancy	
Sr1	0	1/2	0.1935(3)	1.0	
Sr2	0	1/2	0.4211(2)	1.0	
Sc	1/2	0	0.3188(5)	1.0	
O1	1/2	1/2	0.2795(8)	1.0	
O2	1/2	0	0.422(2)	1.0	
Co	1/2	1/2	0	1.0	
As	1/2	0	0.0881(3)	1.0	

the long-range order, should become weak when the distance of CoAs layers becomes large.

B. Magnetization and electric resistivity

Figure 3(a) shows temperature dependence of M in $H = 1, 10, 30, 50,$ and 70 kOe , and Fig. 3(b) shows H dependence of M at various temperatures. From the behavior of the magnetization in the figures, one can find our sample being

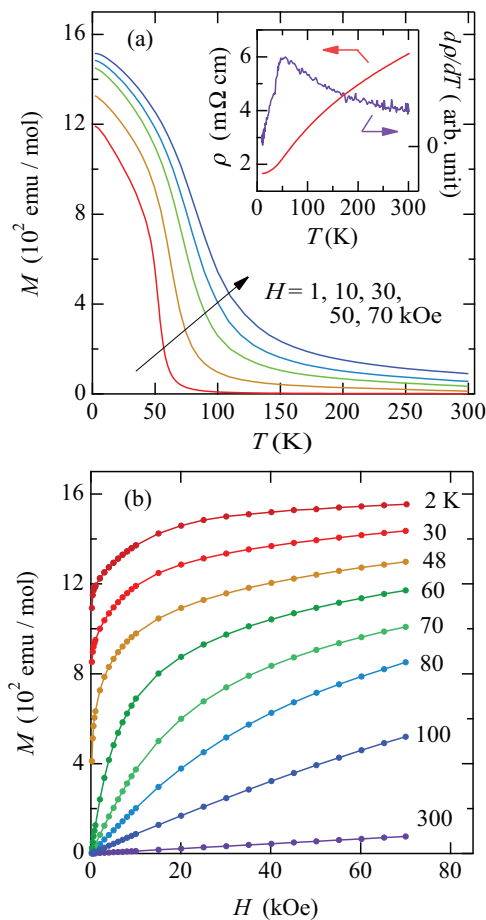


FIG. 3. (Color online) (a) T dependence of M at $H = 1, 10, 30, 50,$ and 70 kOe . Inset: T dependence of ρ and $d\rho/dT$. (b) Isothermal magnetization curves at various temperatures.

in a ferromagnetic state in the low- T region in spite of a large distance between CoAs layers. The inset of Fig. 3(a) shows temperature dependence of ρ and $d\rho/dT$ of the sample. Clear metallic conductivity was observed as other members with CoAs layers.^{7,16,17} The $d\rho/dT$ shows a peak at about 50 K, which peak corresponds to the ferromagnetic transition since spin fluctuations which scatter conduction electrons are abruptly reduced in the ferromagnetic state. These results show that the ferromagnetic ordering and the electric conductivity simultaneously occur in the CoAs layers as in the case of LaCoAsO. The results of measurements are different from those shown in the previous report.¹⁰ Though we cannot explain the cause of the difference, we think our results are reliable since the quality of our sample is good as shown above. Effects of demagnetization should be taken into account in cases of the usual ferromagnetic compounds. Since our sample shows smaller magnetization than usual ferromagnets, effects of demagnetization are negligible even if one assumes the demagnetizing factor $N = 1$. From this reason, we ignore the effects of demagnetization in this paper.

Usually, the Arrott plot, or the M^2 vs H/M plot, is used to determine the value of T_C , especially in cases of WIF compounds. Figure 4 shows Arrott plots of the sample at various temperatures. We could not observe the linear relations between M^2 and H/M which are expected for usual WIF compounds, but we observe two characteristic behaviors: one is that M^2 draws convex curves around T_C (~ 50 K), and the other is that at $T = 2$ K the data seem to change their slopes around $H/M = 15$ mol Oe/emu. Within the spin fluctuation theory by Takahashi,¹³ the former character can be understood as the critical behavior of the ferromagnetic transition, and we can get spin fluctuation parameters out by analyzing the curves. We will discuss the values of these parameters and the validity of them in the next subsection. The latter character is not understood within Takahashi's theory, since M^2 should obey a linear relation with H/M at the ground state. We presume that this anomaly is due to an anisotropy in the magnetic structure like LaCo₂P₂,¹⁸ but for further discussion, we need a single crystalline sample.

Spontaneous magnetization [M_s ($\equiv M|_{H \rightarrow 0}$)] and magnetic susceptibility [χ ($\equiv M/H|_{H \rightarrow 0}$)] were estimated from

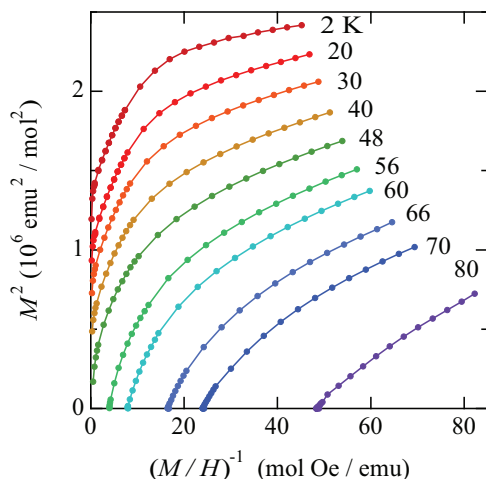


FIG. 4. (Color online) Arrott plots at various temperatures.

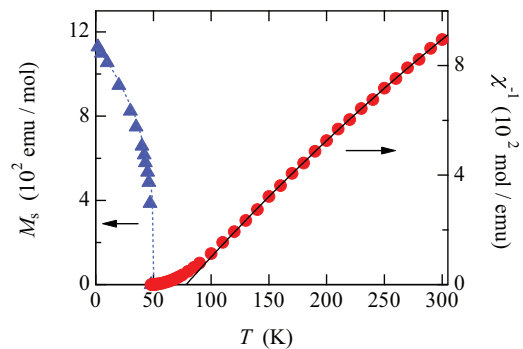


FIG. 5. (Color online) T dependence of M_s (closed triangle) and χ^{-1} (closed circle). Solid line on χ^{-1} shows a result of Curie-Weiss fitting.

the values of intersections of extrapolation of the M^2 - H/M curve and vertical or horizontal axes, respectively. Figure 5 shows the temperature dependence of thus estimated M_s and χ^{-1} . Both M_s and χ^{-1} show typical temperature dependence for WIF. We determined the value of T_C from the figure as the temperature at which both M_s and χ^{-1} take zero: $T_C = 48$ K. The spontaneous magnetization at the ground state was estimated as $P_s = 1129$ emu/mol ($\equiv 0.202\mu_B$) by extrapolating the M_s curve to $T = 0$ K. Here μ_B is the Bohr magneton. The solid line in the figure is the result of fitting the Curie-Weiss law with a constant term χ_0 to χ^{-1} above 130 K. By this analysis, the effective Bohr magneton number, the Weiss temperature, and the constant term were determined as $P_{\text{eff}} = 1.30\mu_B$, $\theta = 78$ K, and $\chi_0 = 1.63 \times 10^{-4}$ emu/mol, respectively. The ratio of P_{eff}/P_s , which indicates the degree of itinerancy of magnetic moments, is 6.5. This value is larger than the value of ~ 1 which is for the case of localized magnetic moments. Sr₂ScO₃CoAs is therefore an itinerant electronic ferromagnet and can be categorized as a WIF. These magnetic parameters are listed in Table II.

Magnetic interaction between CoAs layers is necessary for long-range ordering at finite temperature. In cases of high- T_C cuprates, the interlayer molecular field is enhanced through development of in-plane magnetic susceptibility.^{19–22} This fact shows that if magnetic moments within a plane strongly interact with each other and behave as “giant magnetic moments,” magnetic interaction between such giant magnetic moments can stabilize three-dimensional ordering at finite temperature, even if the interlayer interaction is quite weak as compared with its strength expected from the transition temperature. We would like to note that for a ferromagnetic case, magnetic dipole interaction cannot be ignored. In our tentative calculation for Sr₂ScO₃CoAs, with an assumption that each ferromagnetic domain is in a size of $1 \mu\text{m}^2$ in CoAs layers and magnetic dipole interaction works between

TABLE II. Magnetic parameters of Sr₂ScO₃CoAs and LaCoAsO for comparison (Ref. 9).

	T_C (K)	θ (K)	P_{eff} (μ_B)	P_s (μ_B)	P_{eff}/P_s
Sr ₂ ScO ₃ CoAs	48	78	1.30	0.202	6.5
LaCoAsO	55	98.4	1.34	0.28	4.8

them, stabilization energy due to this interaction becomes large enough for making the system order at finite temperatures. Three-dimensional ferromagnetic transition of $\text{Sr}_2\text{ScO}_3\text{CoAs}$ is therefore driven by two-dimensional magnetic interaction within CoAs layers and is supported by weak interlayer magnetic interaction, possibly a classical magnetic dipole interaction. In such a case, ordered magnetic moments are expected to align along the c axis according to simple electromagnetism. The same logic can apply to other members of the family with CoAs layers. In the case of LaCoAsO , a member of the family, ordered magnetic moments have been reported to align along the c axis,²³ indicating correctness of the above scenario. The same magnetic structure is therefore expected for $\text{Sr}_2\text{ScO}_3\text{CoAs}$, and the anomaly observed in the Arrott plot at $T = 2$ K is possibly due to such an anisotropic magnetic structure.

$\text{Sr}_2\text{ScO}_3\text{CoAs}$ resembles LaCoAsO in magnetism as shown in Table II and also in the value of lattice parameter a . These resemblances indicate that magnetism of these two compounds depends only on the electronic structure within CoAs layers and is not sensitive to the distance between CoAs layers. Therefore suppression of ferromagnetic ordering is difficult to achieve by increasing the distance between CoAs layers. On the other hand, suppression of ferromagnetism is expected to be achieved by decreasing lattice parameter a as in the case of three-dimensional WIFs. If ferromagnetic ordering is completely suppressed by compression along a axis and the system reaches the quantum critical point, a pure two-dimensional nature is possibly observed. For this reason, it must be interesting to study compounds with the value of a smaller than $\text{Sr}_2\text{ScO}_3\text{CoAs}$.

C. Analyses based on the spin-fluctuation theory

In the spin-fluctuation theory for WIF, a spin-fluctuation spectrum of a system is in a form of double Lorentzian function and the magnetism of the system is determined by the width of the spectrum.^{12,24} T_A , T_0 , and F_1 are important parameters in this theory, where T_A and T_0 are, in K, related to the width of the spin-fluctuation spectrum along wave-number direction and along the frequency direction, respectively. F_1 is, also in K, related to the fourth coefficient of the Landau expansion of free energy of the system. According to Takahashi,¹³ it is also determined as $F_1 = g^2 T_A^2 / 15 T_0$, where $g = 2$. We analyzed the magnetization of $\text{Sr}_2\text{ScO}_3\text{CoAs}$ based on this theory.

We first estimated the value of the critical exponent δ by fitting $M \propto H^{1/\delta}$ to the low- H region of the M vs H curve at T_C as $\delta = 5.02$, a value larger than those of three-dimensional Heisenberg and three-dimensional Ising models ($\delta \sim 4.81$),²⁵ and much smaller than that of the two-dimensional Ising model ($\delta = 15$).²⁶ In Takahashi's theory, a linear relation between M^4 and H/M are predicted at T_C due to the ferromagnetic critical behavior. This relation is expressed with T_A as¹³

$$M^4 = 1.86 \times 10^{19} (T_C^2 / T_A^3) (H/M). \quad (1)$$

This means that the value of δ in the system for which Takahashi's theory is adapted is 5, which indicates the validity of this theory for $\text{Sr}_2\text{ScO}_3\text{CoAs}$. Figure 6 shows M^4 at T_C plotted against H/M . Although the data follow a convex curve

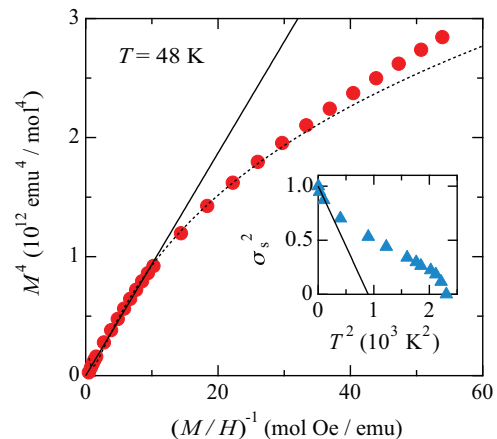


FIG. 6. (Color online) H/M dependence of M^4 at $T = T_C$. Solid line is a result of a linear fitting of Eq. (1) to the data. Dotted line is a result of fitting of $[\ln(H/M)]^2$ to the data (see text). Inset: T^2 dependence of σ_s^2 [$=M_s(T)^2/M_s(0)^2$]. Solid line is a result of calculation by Eq. (3) using the value of T_A obtained from M^4 vs H/M plot.

rather than a straight line, in the low- H (low- H/M) region the data show linearity. This behavior is consistent with the value of δ observed in the low- H region as discussed above. The value of T_A was estimated by fitting Eq. (1) to the low- H/M region of the data as 7.71×10^3 K. Putting the values of T_A , T_C , and P_s in the equation,

$$T_C = (60c)^{-3/4} P_s^{3/2} T_A^{3/4} T_0^{1/4}, \quad (2)$$

we obtained the value of T_0 as 1389 K. Here c is a constant equal to 0.3353... By putting the values of T_A and T_0 in $F_1 = g^2 T_A^2 / 15 T_0$, we estimated the value of F_1 as 11.4×10^3 K. The values of spin-fluctuation parameters are listed in Table III.

The parameter T_A also appears in temperature dependence of spontaneous magnetization near the ground state as

$$\sigma_s^2 = 1 - \frac{a_0}{P_s^4 T_A^2} T^2, \quad (3)$$

where $a_0 = 112.1 \dots$ and $\sigma_s = M_s(T)/M_s(0)$.^{13,27} In the inset of Fig. 6 we show the σ_s^2 vs T^2 plot together with the result of a calculation by Eq. (3) using the values of T_A and P_s obtained above. The calculated result well explains the experimental data, showing validity of the estimation of T_A . F_1 also appears in the slope of the Arrott plot at the ground state as $N_0^3 (g\mu_B)^4 / k_B F_1$, where N_0 is the number of magnetic atoms in a sample. The value of F_1 estimated by fitting this equation to the Arrott plot at 2 K above 15 mol Oe/emu is 22.6×10^3 K. One can consider this value consistent

TABLE III. Spin-fluctuation parameters of $\text{Sr}_2\text{ScO}_3\text{CoAs}$ together with those of LaCoAsO (Ref. 9). Values of F_1 are those estimated from the equation $F_1 = g^2 T_A^2 / 15 T_0$.

	T_A (10^3 K)	T_0 (K)	F_1 (10^3 K)	T_C/T_0
$\text{Sr}_2\text{ScO}_3\text{CoAs}$	7.71	1389	11.4	0.035
LaCoAsO	6.21	644	16.0	0.085

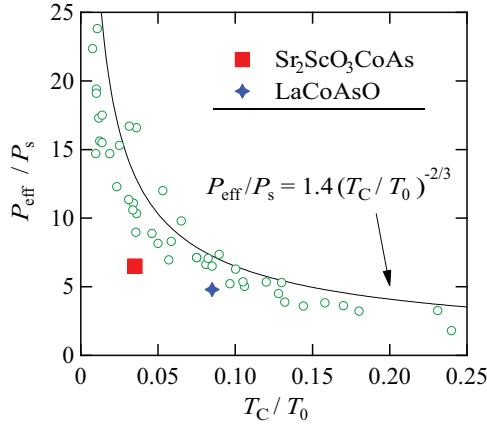


FIG. 7. (Color online) Takahashi-Rhodes-Wohlfarth plot. Data shown by small opened circles are reproduced from Ref. 13 and references therein. Data of LaCoAsO are reproduced from Ref. 9.

with the value obtained from T_A and T_0 . The result of these crosschecks shows that we successfully obtained the spin fluctuation parameters consistently. As shown in Table III, spin-fluctuation parameters of $\text{Sr}_2\text{ScO}_3\text{CoAs}$ are different from those of LaCoAsO although static magnetic parameters, especially T_C and P_{eff} , are similar to each other. It should be noted that the value of T_0 is double compared with that of LaCoAsO, from which we suggest that destabilization of magnetic ordering due to enhancement of two-dimensionality proceeds in $\text{Sr}_2\text{ScO}_3\text{CoAs}$.

The ratios of P_{eff}/P_s and T_C/T_0 should obey the relation $P_{\text{eff}}/P_s = 1.4 \times (T_C/T_0)^{-2/3}$ when a system is three-dimensional WIF.¹³ We plotted P_{eff}/P_s against T_C/T_0 in Fig. 7 to evaluate magnetism of $\text{Sr}_2\text{ScO}_3\text{CoAs}$. As observed in the figure, the data of $\text{Sr}_2\text{ScO}_3\text{CoAs}$ are a bit far from the theoretical curve. This shows that the model of three-dimensional WIFs can be used to explain most magnetism of $\text{Sr}_2\text{ScO}_3\text{CoAs}$ but needs to be corrected slightly in order to explain it completely. We also plotted the data of LaCoAsO. One can see that $\text{Sr}_2\text{ScO}_3\text{CoAs}$ is closer to the ferromagnetic quantum critical point than LaCoAsO. When a system is quasi-two-dimensional WIF, the value of P_{eff}/P_s tends to reduce.¹⁴ Deviation from the theoretical curve for three-dimensional WIF indicates an appearance of quasi-two-dimensional character.

By using spin-fluctuation parameters and magnetic parameters, one can calculate magnetic susceptibility as a function of temperature.^{9,13} Figure 8 shows the result of calculation (black line) by using parameters in Tables II and III together with experimental χ^{-1} (open circles). The inset of the figure shows the magnification of the main panel around T_C . The calculated data are not in agreement with the experimental ones except for the narrow region close to T_C . We therefore supposed that magnetism of $\text{Sr}_2\text{ScO}_3\text{CoAs}$ just around T_C can be understood using the theory of three-dimensional WIF, and it needs modification taking account of the quasi-two-dimensionality for overall explanation of magnetism above T_C .

Finally, we pointed out possible appearances of quasi-two-dimensional character of $\text{Sr}_2\text{ScO}_3\text{CoAs}$. In Fig. 8, we showed a result of fitting of the equation for two-dimensional WIF, $\chi^{-1} = 2T_A(T/6T_0)^{2/3} \times \exp(-P_s^2 T_A/10T)$, to the experimental χ^{-1} as a purple line.^{28,29} The result of calculation is well

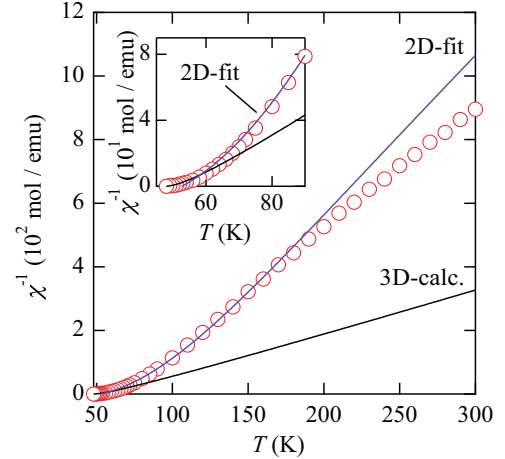


FIG. 8. (Color online) Black line shows calculated results of χ^{-1} based on Refs. 9 and 13. Open circles are the experimental χ^{-1} . Purple line is a result of fitting of equation for two-dimensional ferromagnetic case (Ref. 28). Inset: magnification of the main panel around T_C .

fitted to the data, indicating an appearance of two-dimensional character of $\text{Sr}_2\text{ScO}_3\text{CoAs}$. From the fitting, T_A and T_0 are estimated as $T_A = 52.5 \times 10^3$ K and $T_0 = 16.5 \times 10^3$ K, respectively. These values are almost 10 times larger than the values listed in Table III. This problem should be solved in the future. If magnetic interaction is highly two-dimensional, H/M is proportional to $\exp(M^2)$ at T_C ,¹⁴ and thus M^4 is proportional to $[\ln(H/M)]^2$. In the main panel of Fig. 6, we showed a result of fitting $[\ln(H/M)]^2$ to the data as a dotted line. As observed in the figure, the fitting curve well fits the data in much wider range of H/M than Eq. (1). Thus nonlinearity of the M^4 vs H/M curve also indicates an appearance of quasi-two-dimensional character of $\text{Sr}_2\text{ScO}_3\text{CoAs}$. We can show several collateral evidences of quasi-two-dimensionality of this compound as discussed above. We believe that we can show direct evidences of it if we obtain a single crystalline sample of $\text{Sr}_2\text{ScO}_3\text{CoAs}$.

IV. CONCLUSION

In summary, we successfully synthesized a polycrystalline sample of $\text{Sr}_2\text{ScO}_3\text{CoAs}$ and revealed that this compound shows itinerant electronic ferromagnetism with the Curie temperature $T_C = 48$ K in spite of a large interlayer distance of CoAs layers. We showed magnetism of $\text{Sr}_2\text{ScO}_3\text{CoAs}$ is explained by three-dimensional spin-fluctuation theory around and below T_C and also pointed out the possibility of the realization of quasi-two-dimensional nature in magnetism.

ACKNOWLEDGMENTS

We would like to thank Prof. H. Takagi for allowing us to use the MPMS. This work was supported by a Grant-in-Aid for Young Scientists (B) from the Japan Society for the Promotion of Science (Grant No. 24760534).

*h-ohta@cc.tuat.ac.jp

†h-katori@cc.tuat.ac.jp

- ¹T. Waki, S. Terazawa, Y. Tabata, F. Oba, C. Michioka, K. Yoshimura, S. Ikeda, H. Kobayashi, K. Ohoyama, and H. Nakamura, *J. Phys. Soc. Jpn.* **79**, 043701 (2010).
- ²T. Waki, Y. Umemoto, S. Terazawa, Y. Tabata, A. Kondo, K. Sato, K. Kindo, S. Alconchel, F. Sapiña, Y. Takahashi, and H. Nakamura, *J. Phys. Soc. Jpn.* **79**, 093703 (2010).
- ³N. T. Huy, A. Gasparini, D. E. de Nijs, Y. Huang, J. C. P. Klaasse, T. Gortemulder, A. de Visser, A. Hamann, T. Görlach, and H. v. Löhneysen, *Phys. Rev. Lett.* **99**, 067006 (2007).
- ⁴T. Ohta, T. Hattori, K. Ishida, Y. Nakai, E. Osaki, K. Deguchi, N. K. Sato, and I. Satoh, *J. Phys. Soc. Jpn.* **79**, 023707 (2010).
- ⁵T. Hattori, Y. Ihara, Y. Nakai, K. Ishida, Y. Tada, S. Fujimoto, N. Kawakami, E. Osaki, K. Deguchi, N. K. Sato, and I. Satoh, *Phys. Rev. Lett.* **108**, 066403 (2012).
- ⁶Y. Kamihara, T. Watanabe, M. Hirano, and H. Hosono, *J. Am. Chem. Soc.* **130**, 3296 (2008).
- ⁷H. Yanagi, R. Kawamura, T. Kamiya, Y. Kamihara, M. Hirano, T. Nakamura, H. Osawa, and H. Hosono, *Phys. Rev. B* **77**, 224431 (2008).
- ⁸A. S. Sefat, A. Huq, M. A. McGuire, R. Jin, B. C. Sales, D. Mandrus, L. M. D. Cranswick, P. W. Stephens, and K. H. Stone, *Phys. Rev. B* **78**, 104505 (2008).
- ⁹H. Ohta and K. Yoshimura, *Phys. Rev. B* **79**, 184407 (2009).
- ¹⁰Y. L. Xie, R. H. Liu, T. Wu, G. Wu, Y. A. Song, D. Tan, X. F. Wang, H. Chen, J. J. Ying, Y. J. Yan, Q. J. Li, and X. H. Chen, *Europhys. Lett.* **86**, 57007 (2009).
- ¹¹F. L. Ning, K. Ahilan, T. Imai, A. S. Sefat, M. A. McGuire, B. C. Sales, D. Mandrus, P. Cheng, B. Shen, and H. H. Wen, *Phys. Rev. Lett.* **104**, 037001 (2010).
- ¹²T. Moriya, *Spin Fluctuations in Itinerant Electron Magnetism* (Springer-Verlag, New York, 1985).
- ¹³Y. Takahashi, *J. Phys. Soc. Jpn.* **55**, 3553 (1986).
- ¹⁴Y. Takahashi, *J. Phys.: Condens. Matter* **9**, 10359 (1997).
- ¹⁵F. Izumi and K. Momma, *Solid State Phenom.* **130**, 15 (2007).
- ¹⁶M. A. McGuire, D. J. Gout, V. O. Garlea, A. S. Sefat, B. C. Sales, and D. Mandrus, *Phys. Rev. B* **81**, 104405 (2010).
- ¹⁷H. Ohta, C. Michioka, and K. Yoshimura, *Phys. Rev. B* **84**, 134411 (2011).
- ¹⁸M. Reehuis, C. Ritter, R. Ballou, and W. Jeitschko, *J. Magn. Magn. Mater.* **138**, 85 (1994).
- ¹⁹J. M. Tranquada, G. Shirane, B. Keimer, S. Shamoto, and M. Sato, *Phys. Rev. B* **40**, 4503 (1989).
- ²⁰J. M. Tranquada, P. M. Gehring, G. Shirane, S. Shamoto, and M. Sato, *Phys. Rev. B* **46**, 5561 (1992).
- ²¹R. Stern, M. Mali, I. Mangelschots, J. Roos, D. Brinkmann, J. Y. Genoud, T. Graf, and J. Muller, *Phys. Rev. B* **50**, 426 (1994).
- ²²A. J. Millis and H. Monien, *Phys. Rev. B* **54**, 16172 (1996).
- ²³J. Sugiyama, M. Månsson, O. Ofer, K. Kamazawa, M. Harada, D. Andreica, A. Amato, J. H. Brewer, E. J. Ansaldo, H. Ohta, C. Michioka, and K. Yoshimura, *Phys. Rev. B* **84**, 184421 (2011).
- ²⁴Y. Takahashi and T. Moriya, *J. Phys. Soc. Jpn.* **54**, 1592 (1985).
- ²⁵J. C. Le Guillou and J. Zinn-Justin, *Phys. Rev. Lett.* **39**, 95 (1977).
- ²⁶D. S. Gaunt, M. E. Fisher, M. F. Sykes, and J. W. Essam, *Phys. Rev. Lett.* **13**, 713 (1964).
- ²⁷K. Shimizu, H. Maruyama, H. Yamazaki, and H. Watanabe, *J. Phys. Soc. Jpn.* **59**, 305 (1990).
- ²⁸M. Hatatani and T. Moriya, *J. Phys. Soc. Jpn.* **64**, 3434 (1995).
- ²⁹H. Sugawara, K. Ishida, Y. Nakai, H. Yanagi, T. Kamiya, Y. Kamihara, M. Hirano, and H. Hosono, *J. Phys. Soc. Jpn.* **78**, 113705 (2009).